

Effect of orientation on cyclic stress–strain curves and dislocation patterns of Ag and Cu single crystals

P. Li, Z.F. Zhang*, S.X. Li, Z.G. Wang

Shenyang National Laboratory for Materials Science, Institute of Metal Research, Chinese Academy of Sciences, 72 Wenhua Road, Liaoning 110016, Shenyang, PR China

ARTICLE INFO

Article history:

Received 27 October 2009

Received in revised form

25 November 2009

Accepted 10 December 2009

Keywords:

Ag single crystal

Cu single crystal

Orientation

Cyclic deformation

Persistent slip bands (PSBs)

Dislocation patterns

ABSTRACT

Cu and Ag single crystals with different orientations show great similarities in their cyclic deformation behavior, including cyclic stress–strain (CSS) curves and dislocation patterns. Based on a large amount of experimental results, it is found that single-slip, conjugate double-slip and $[0\ 1\ 1]$ multiple-slip oriented Cu and Ag single crystals exhibit obvious plateau behavior in their CSS curves and the corresponding dislocation patterns are composed of typical two-phase structure including persistent slip bands (PSBs) and veins. However, the critical and coplanar double-slip oriented Cu and Ag single crystals do not exhibit clear plateau region in their CSS curves and labyrinth and cell structures are typical due to the different dislocation reactions. The relationship between the CSS curves and the saturation dislocation patterns was discussed and summarized.

© 2010 Elsevier B.V. All rights reserved.

1. Introduction

It is well known that cyclic deformation behavior of face-centered-cubic (fcc) single crystals had been widely studied since “persistent slip band” (PSB) was defined as the common characteristics of fatigued crystals by Thompson et al. [1]. Subsequently, a large number of researchers focused on various PSBs’ mechanical and structural characteristics, including hardness, distribution, volume fraction, two-phase model and so on [2–7]. In 1978, Mughrabi established the famous cyclic stress–strain (CSS) curve of single-slip-oriented Cu single crystal over a wide range of plastic strain amplitudes, which showed a clear plateau behavior with the plateau stress amplitude of ~ 28 MPa. Thereafter, Cheng and Laird [8] found that for most single-slip oriented Cu single crystals their saturation stress amplitudes at room temperature are in the range of 28–30 MPa.

Based on the results of single-slip oriented Cu single crystals, different double-slip oriented Cu single crystals as well as multiple-slip oriented ones are investigated in succession. Firstly, Jin and Winter [9–12] studied systematically the CSS responses and dislocation arrangements of Cu single crystals with $[0\ 1\ 2]$, $[\bar{1}\ 1\ 2]$ and $[\bar{1}\ 2\ 2]$ double-slip orientations on the three sides of the standard stereographic triangle at a relatively high strain amplitude of

3.0×10^{-3} . They found that different regions in the stereographic triangle corresponded to different dislocation interaction models and cyclic deformation behavior. Secondly, Gong et al. [13,14] and Lepisto et al. [15–17] studied the cyclic deformation behavior of $[0\ 0\ 1]$ and $[\bar{1}\ 1\ 1]$ multiple-slip oriented Cu single crystals, respectively. The results showed that the plateau behavior in multiple-slip oriented Cu single crystals disappeared. In $[0\ 0\ 1]$ Cu single crystals after cyclic saturation, the labyrinth structure is easier to form. And in $[\bar{1}\ 1\ 1]$ Cu single crystals after cyclic saturation, the cell structure is more often to be seen. Later, Li et al. [18] systematically summarized the cyclic deformation behavior of $[0\ 1\ 1]$ Cu single crystals. They found that the plateau behavior also appeared in $[0\ 1\ 1]$ Cu single crystals, which is similar to that of single-slip oriented one. Based on a plenty of experimental results from different oriented Cu single crystals, Li et al. [19–24] proposed a general conclusion on orientation effect of Cu single crystals. They suggested that when the crystallographic orientation changes from single-slip orientation to double-slip orientation, even to multiple-slip orientations, the plateau behavior of Cu single crystals will gradually disappear and the saturation resolved shear stress will increase obviously, especially at higher strain amplitude.

All in all, the macroscopic deformation behavior in fcc crystals depends on their microscopic dislocation structures. Therefore, it is necessary to further summarize the classical dislocation configurations in differently oriented fcc single crystals. In our previous paper [25], we have compared the CSS curves and surface slip morphologies in fatigued Ag and Cu single crystals with different orientations

* Corresponding author. Tel.: +86 24 23971043.

E-mail address: zhfzhang@imr.ac.cn (Z.F. Zhang).

and found that the cyclic deformation behavior between Ag and Cu single crystals shows many similarities. In order to more deeply understand the regularity of orientation effect, more oriented Ag single crystals will be selected as model materials. After systematically investigating the effect of orientation on CSS curves and dislocation configurations of Ag single crystals and comparing the results with those of similarly oriented Cu single crystals, some common principles on orientation effect will be expected to be made.

2. Experimental procedures

All Ag single crystals with different orientations were grown from electrolytic Ag of 99.999% purity by the Bridgman method. The crystal orientations (G) were determined by the electron back-scattering diffraction (EBSD) technique in a Cambridge S360 scanning electron microscope (SEM), as shown in Fig. 1. The fatigue specimens with dimensions of 7 mm \times 5 mm \times 54 mm and a gauge section of 5 mm \times 5 mm \times 16 mm were cut by an electron-spark cutting machine. Cu single crystals with different orientations are also shown in Fig. 1 for comparison. The detailed experimental procedures, including the preparation of fatigue specimens and the fatigue test procedure at constant plastic strain amplitudes, can be found in relevant references [18,26–30]. After the fatigue tests, the dislocation arrangements were carefully observed by the electron channeling contrast (ECC) technique in a Cambridge S360 SEM. Such ECC images are similar in appearance to transmission electron micrographs, albeit with a lower image resolution [31–34]. In particular, this technique not only can provide a real and wide view of dislocation substructures conveniently, but also makes it possible to establish the relationship between dislocation arrangements and crystallographic characterization of the deformed crystals at some special sites, such as PSBs [31–34], grain boundaries [35–37] and the front of the crack [38,39].

3. Results and discussion

3.1. CSS curves of Cu and Ag single crystals with single-slip orientations

Several groups of Cu and Ag single crystals with representative orientations are selected. As shown in Fig. 1, these orientations include single-slip orientation with the highest Schmid factor of ~ 0.5 , coplanar double-slip orientation of $[\bar{2}33]$, conjugate double-slip orientations of $[\bar{1}12]$ and $[\bar{4}59]$, critical double-slip orientations of $[017]$ and $[\bar{1}414]$, and multiple-slip orientation of $[011]$. Detailed fatigue testing conditions and experimental data on cyclic saturation in various Cu and Ag single crystals are summarized in Table 1, where γ_{pl} and τ_s are the plastic shear strain amplitude and saturation resolved shear stress amplitude, respectively. It can be seen from Table 1, the cyclic saturation stress amplitudes of Ag single crystal are generally about 5–10 MPa lower than those of Cu single crystals with the similar orientations, where the difference in value depends on the orientation and strain amplitude in detail. In addition, the CSS curve of single-slip oriented Ag single crystal is mostly composed of the data of $[\bar{1}818]$ Ag single crystal, as shown in Fig. 2. The Schmid factor of $[\bar{1}818]$ Ag single crystal is $\Omega = 0.498$, which is comparable with the single-slip-oriented Cu single crystal with Schmid factor of $\Omega = 0.5$. The data in Table 1 provide detailed base for the establishment of the CSS curves. In the following, single-slip orientation will be firstly mentioned.

From our recent study [30], it is known that the plateau region also appeared in the CSS curve of single-slip oriented Ag single crystal. As shown in Fig. 2, the CSS curve of Ag single crystal shows

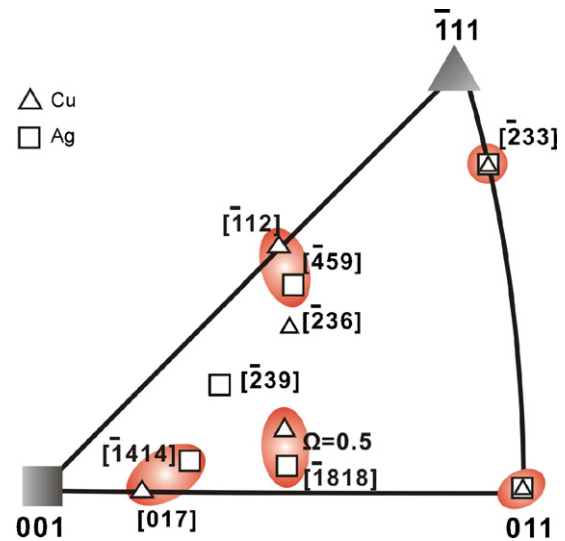


Fig. 1. Stereographic triangle showing the orientations of loading axis for Cu and Ag single crystals involved in this paper, where Cu single crystals with different orientations are taken from Mughrabi [26] and Li et al. [18,27–29], respectively.

evident three stages. However, as compared with Cu single crystal, the plateau stress of Ag single crystal decreased. The plateau stress of Cu single crystal with single-slip orientations is ~ 28 MPa, but it is ~ 20 MPa for $[\bar{1}818]$ Ag single crystal. Meanwhile it should be pointed out that at the shear strain amplitude higher than $\gamma_{pl} \geq 1.0 \times 10^{-3}$, the cyclic saturation stresses of Ag single crystals are somewhat higher than those at lower strain amplitudes, which is different from Cu single crystal. Mughrabi [40] suggested that the difference in the stacking fault energy (SFE) between Cu and Ag may be the main reason for this phenomenon. Indeed Cu and Ag single crystals with single-slip orientations show certain similarity, but not fully. Therefore it is necessary to make further comparison among double-, multiple- and single-slip oriented Cu and Ag single crystals.

3.2. CSS curves of double- and multiple-slip-oriented Cu or Ag single crystals

Fig. 3 shows the CSS curves of Cu and Ag single crystals with different orientations. Firstly, as shown in Fig. 3(a), for coplanar double-slip oriented single crystals of Cu or Ag, their CSS curves show a quasi-plateau behavior characterized with three stages. On

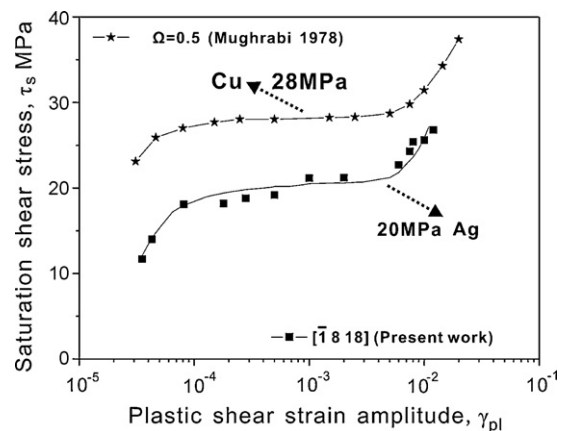


Fig. 2. CSS curves of single-slip oriented Cu and Ag single crystals. Single-slip oriented Cu single crystals with Schmid factor $\Omega = 0.5$ come from Mughrabi [26] and $[\bar{1}818]$ single-slip oriented Ag single crystals are from the present work.

the other hand, in the quasi-plateau region, the saturation stresses are obviously higher than those of single-slip oriented Cu or Ag single crystals. By comparison, it can be seen that in the range of the plateau region the increase in the saturation stress of Ag single crystal with coplanar double-slip orientation is more average. However, for Cu single crystals, Li et al. [27] found that the difference in the saturation stress between coplanar double-slip and single-slip orientations is gradually increasing with increasing the strain amplitude. Anyhow at least near the strain amplitude of 2×10^{-3} , the saturation stress of coplanar double-slip orientations is 5–6 MPa higher than those of their respective single-slip orientations (see Table 1).

Fig. 3(b) shows the CSS curves of the conjugate double-slip oriented Cu and Ag single crystals. Their plateau behavior is similar to that of the single-slip orientations with the same plateau stress, except that the strain range of the corresponding plateau region is a little short. Therefore, the plateau stresses of the conjugate double-slip oriented Cu and Ag single crystals are still 28 MPa and 20 MPa, respectively. Jin et al. [9,10] found that the saturation stress of $[\bar{1}12]$ Cu single crystal is 28.3 MPa at the strain amplitude of $\gamma_{pl} = 3.0 \times 10^{-3}$. The narrowing of the plateau region indicates that the dislocation reaction may be easier for conjugate double-slip oriented fcc single crystals, which will cause the further evolution of dislocation patterns.

The CSS curves of critical double-slip oriented Cu and Ag single crystals are shown in Fig. 3(c). In the plateau region, the saturation stresses are distinctly higher than those of their respective single-slip orientations. In critical double-slip oriented Cu and Ag single

crystals, the CSS curve of $[\bar{1}414]$ Ag single crystal presents more clear plateau behavior, but for $[017]$ Cu single crystal the plateau behavior is invisible and the saturation stress is gradually increasing with increasing the strain amplitude, which is similar to the finding in $[\bar{2}33]$ Cu single crystal [27]. According to the division of the stereographic triangle by Jin et al. [9,10], it can be understood that $[\bar{1}414]$ orientation is much closer to the single-slip region than $[017]$ orientation [41]. In fact, the orientation division based on the dislocation reaction is not very strict, which is only a qualitative representation. Just as pointed out by Jin et al. [9,10], the division of the stereographic triangle changes with the plastic strain amplitude. The higher the strain amplitude is, the smaller the single-slip region becomes and the larger the double- and multiple-slip regions become. Thus, the division of the orientation region in the stereographic triangle should be established based on the detailed comparison of the saturation stresses and more observations of dislocation arrangements.

Three groups of typical double-slip orientations present their respective cyclic deformation behavior. In the following, one of the classical multiple-slip orientation $[011]$ will be introduced because this orientation has its own specificity with respect to the plateau behavior of the CSS curve. Although a number of slip systems are easy to operate in $[011]$ crystal, their operation becomes active only after the strain amplitude reaches a certain value [18]. As long as the applied strain amplitude is not too high, dislocation movement in $[011]$ crystal is still mainly on the primary slip system, resulting in the two-phase structure of PSBs and veins. It is well known that the determination of the orientation is usually an

Table 1

Fatigue testing conditions and data for Cu and Ag single crystals with different orientations. (Note: the data of Cu single crystals are from the extensive works [18,26–29].).

Copper	Specimen no.	γ_{pl}	Cycles	τ_s (MPa)	Silver	Specimen no.	γ_{pl}	Cycles	τ_s (MPa)
<i>Single-slip orientation</i>									
$\Omega = 0.5$	1	3.1×10^{-5}	227,580	23.1	$[\bar{1}818]$	1	3.5×10^{-5}	200,000	11.7
	2	4.65×10^{-5}	216,560	25.9		2	4.3×10^{-5}	180,000	14
	3	8.0×10^{-5}	162,500	26.6		3	8.1×10^{-5}	150,000	18.1
	4	1.5×10^{-4}	46,000	27.7		4	1.8×10^{-4}	120,000	18.2
	5	2.5×10^{-4}	15,550	28.04		5	2.8×10^{-4}	100,000	18.8
	6	5.0×10^{-4}	20,495	28.04		6	5.0×10^{-4}	80,000	19.2
	7	1.5×10^{-3}	4733	28.24		7	1.0×10^{-3}	50,000	21.16
	8	2.5×10^{-3}	2480	28.3		8	2.0×10^{-3}	20,000	21.2
	9	5.05×10^{-3}	3683	28.7		9	6.0×10^{-3}	10,000	22.7
	10	7.5×10^{-3}	3365	29.8		10	7.5×10^{-3}	8000	24.3
	11	1.0×10^{-2}	656	31.44		11	8.0×10^{-3}	8000	25.4
	12	1.45×10^{-2}	474	34.3		12	1.0×10^{-2}	6000	25.6
	13	2.0×10^{-2}	313	37.4		13	1.2×10^{-2}	4000	26.8
<i>Coplanar double-slip orientation</i>									
$[\bar{2}33]$	1	1.3×10^{-4}	65,000	25.0	$[\bar{2}33]$	1	1.35×10^{-4}	20,000	24.5
	2	6.2×10^{-4}	22,500	30.9		2	6.7×10^{-4}	10,000	25.4
	3	1.7×10^{-3}	6000	32.5		3	1.35×10^{-3}	5000	23.3
	4	3.5×10^{-3}	4700	33.5		4	2.7×10^{-3}	4000	27.2
	5	7.5×10^{-3}	17,560	37.2		5	8.1×10^{-3}	2000	32
<i>Conjugate double-slip orientation</i>									
$[\bar{1}12]$	1	1.4×10^{-3}	9100	28.6	$[\bar{4}59]$	1	1.15×10^{-3}	50,000	21.01
	2	2.3×10^{-3}	7100	28.7		2	2.3×10^{-3}	20,000	21.31
	3	3.3×10^{-3}	7000	28.2		3	3.45×10^{-3}	15,000	22.71
	4	4.9×10^{-3}	14,000	29.6		4	4.6×10^{-3}	2500	24.53
<i>Critical double-slip orientation</i>									
$[017]$	1	1.2×10^{-4}	84,100	28.6	$[\bar{1}414]$	1	1.0×10^{-4}	50,000	23.2
	2	3.0×10^{-4}	38,200	34.2		2	1.5×10^{-4}	40,000	25.2
	3	7.0×10^{-4}	20,000	36.7		3	5.0×10^{-4}	20,000	26.6
	4	9.4×10^{-3}	24,000	37.1		4	1.0×10^{-3}	10,000	26.6
	5	1.5×10^{-3}	18,000	38.8		5	2.0×10^{-3}	4000	26.5
	6	5.2×10^{-3}	3600	46.1		6	4.0×10^{-3}	3000	26.65
	7	6.5×10^{-3}	2620	49.2		7	8.0×10^{-3}	2000	28.6
<i>Multiple-slip orientation</i>									
$[011]$	1	1.1×10^{-4}	59,000	29.2	$[011]$	1	1.5×10^{-4}	40,000	19.0
	2	7.3×10^{-4}	16,120	30.7		2	6.1×10^{-4}	20,000	19.4
	3	3.3×10^{-3}	3320	29.9		3	3.7×10^{-3}	10,000	20.7

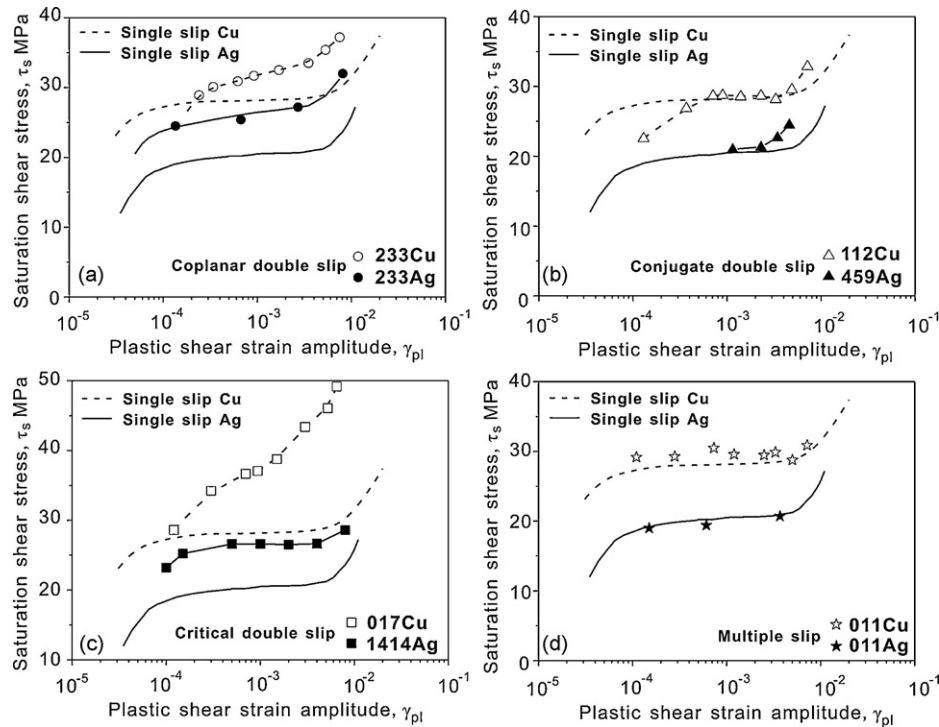


Fig. 3. Comparison of CSS curves between differently oriented Cu and Ag single crystals: (a) coplanar double slip and single slip; (b) conjugate double slip and single slip; (c) critical double slip and single slip; (d) multiple slip and single slip.

approximate value. In this study, this margin of error is about 3°. Even if the determination of the orientation is rather accurate, one primary slip system is always firstly activated in the fcc crystals. Later, according to the difference in the orientation, secondary slip system will begin to operate, either with difficulty or ease. Accordingly, it can be concluded that at low strain amplitudes fcc single crystals undertake the plastic deformation by one primary slip system solely. The actuating of the secondary slip system is caused by the accumulation of plastic deformation.

Until now, the CSS curves of several classical oriented fcc single crystals, including coplanar, conjugate, critical double-slip orien-

tations and [0 1 1] multiple-slip orientation, have already been well summarized. The general trend can be shown as below: (1) the CSS curves of both conjugate double-slip oriented and [0 1 1] multiple-slip oriented Cu or Ag single crystals show obvious plateau behavior and the plateau stresses are consistent with those of respective single-slip-oriented ones. (2) No plateau behavior appears in the coplanar and critical double-slip oriented Cu or Ag single crystals and their saturation stresses gradually increase with the increase in the strain amplitude. But why these double- or multiple-slip oriented Cu and Ag single crystals exhibit different cyclic deformation behaviors? To answer this question,

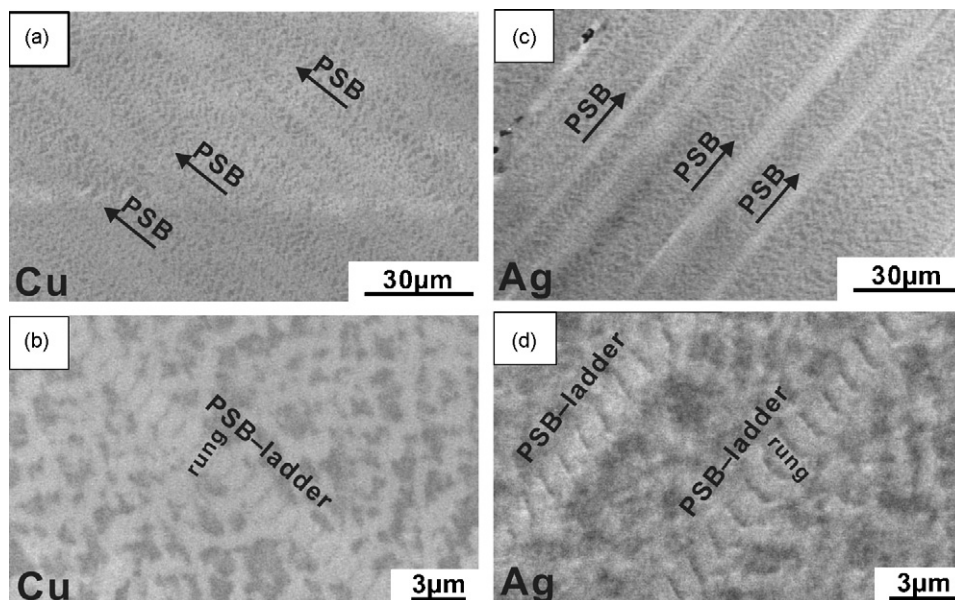


Fig. 4. Dislocation configurations of Cu and Ag single crystals at the plastic resolved shear strain amplitude of $\gamma_{pl} = 2.0 \times 10^{-3}$: (a) and (b) $[\bar{1}39]$ Cu single crystal; (c) and (d) $[\bar{1}818]$ Ag single crystal. (a) and (b) Viewed from $(\bar{2}21)$ plane; (c) and (d) viewed from $(\bar{2}21)$ plane.

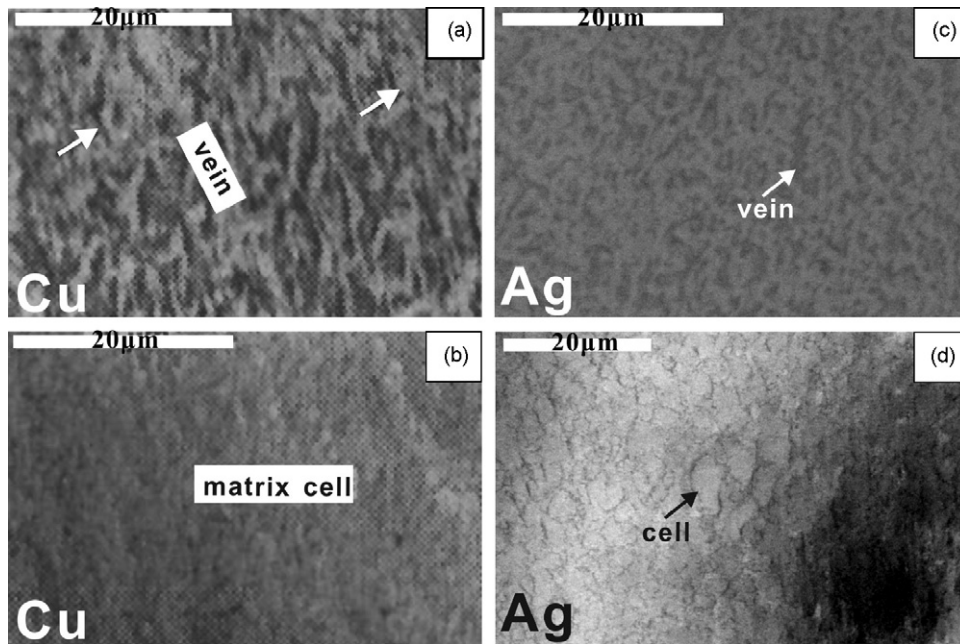


Fig. 5. Dislocation configurations of coplanar double-slip oriented Cu and Ag single crystals: (a) $[\bar{2} 3 3]$ Cu single crystal cycled at $\gamma_{pl} = 6.2 \times 10^{-4}$; (b) $[\bar{2} 3 3]$ Cu single crystal cycled at $\gamma_{pl} = 3.5 \times 10^{-3}$; (c) $[\bar{2} 3 3]$ Ag single crystal cycled at $\gamma_{pl} = 1.35 \times 10^{-4}$; (d) $[\bar{2} 3 3]$ Ag single crystal cycled at $\gamma_{pl} = 8.1 \times 10^{-3}$. (a) and (b) Viewed from $(3 \ 2 \ 0)$ plane; (c) and (d) viewed from $(3 \ 3 \ 1)$ plane. $[\bar{2} 3 3]$ Cu single crystals are from Zhou [42].

the observations of the microscopic dislocation structures will be inevitable.

3.3. Dislocation arrangements of different oriented Cu or Ag single crystals

Fig. 4 presents the classical dislocation arrangements of single-slip-oriented Cu and Ag single crystals. It can be seen from Fig. 4 that the two-phase structure of PSB ladders and matrix veins is the most typical dislocation pattern in the single-slip oriented Cu or Ag single crystals. Mughrabi [26] found that in the plateau region of the CSS curve, the volume fraction of PSBs in the two-phase structure

is constantly increasing with strain amplitude, but the two-phase structure remain unchanged. Thus, it should be repeatedly emphasized that the structural characteristic of dislocation patterns is an intrinsic performance of cyclic deformation behavior in different oriented Cu and Ag single crystals. Then how the dislocation features of other oriented Cu and Ag single crystal are?

It can be realized from Fig. 5 that in the coplanar double-slip oriented Cu and Ag single crystals, most of the saturation dislocation patterns at low strain amplitudes are vein structures, but at higher strain amplitudes the dislocation patterns are dominated by cell structures. For $[\bar{2} 3 3]$ Cu and Ag single crystals, with increasing the strain amplitude, the dislocation configura-

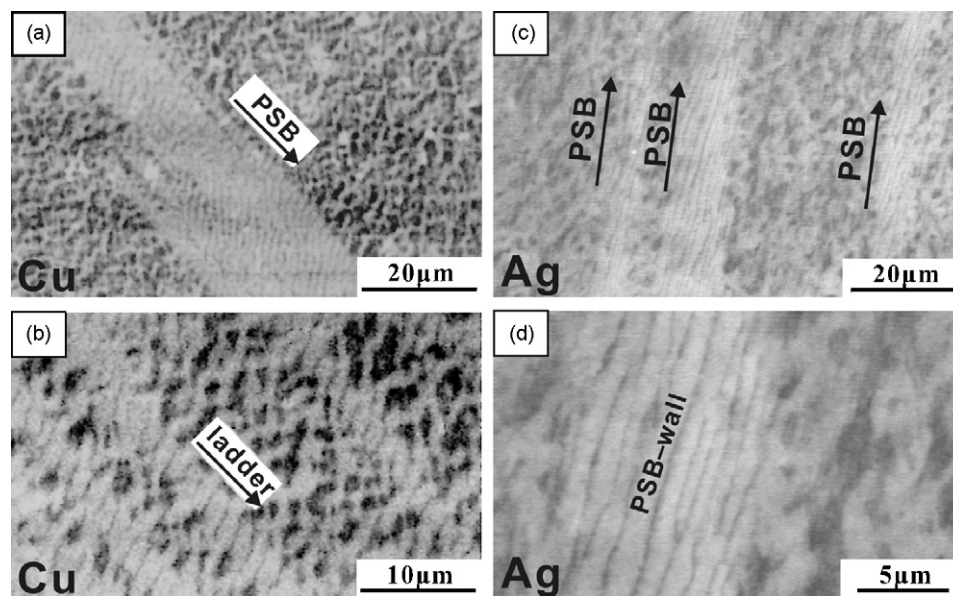


Fig. 6. Dislocation configurations of conjugate double-slip oriented Cu and Ag single crystal at different plastic strain amplitudes: (a) $[\bar{1} 1 2]$ Cu single crystal cycled at $\gamma_{pl} = 3.7 \times 10^{-4}$; (b) $[\bar{1} 1 2]$ Cu single crystal cycled at $\gamma_{pl} = 2.3 \times 10^{-3}$; (c) and (d) $[4 \ 5 \ 9]$ Ag single crystal cycled at $\gamma_{pl} = 4.6 \times 10^{-3}$. (a) and (b) Viewed from $(\bar{2} \ 0 \ 1)$ plane; (c) and (d) viewed from $(1 \ 1 \ 1)$ plane. $[\bar{1} 1 2]$ Cu single crystals are from Li et al. [43].

tions shift naturally from vein to cell structures. In the process of this evolution, no PSB-ladder structure which appears in single-slip oriented single crystals can be found. Therefore, for $[\bar{2}33]$ Cu or Ag single crystals, the formation of cell structure is the most prominent structural feature. Due to the absence of the second-phase structure, these cells are also known as the matrix cell structure according to Zhou [42] by meaning that the cellular structure forms directly from the matrix vein. Together with the CSS curves of coplanar double-slip oriented Cu and Ag single crystals, as shown in Fig. 3(a), it can be found that the absence of PSB-ladder structure makes the plateau behavior no longer clear. On the other hand, the constant formation of cell structure is just the basic factor, which causes the increase in the saturation stress.

Fig. 6 shows the classical dislocation patterns in cyclically saturated Cu and Ag single crystals with conjugate double-slip orientations. In such oriented crystals, the dislocation configurations are still composed of two-phase structure. By careful observation it can be found that on the observation plane $(\bar{2}0\bar{1})$, PSB ladders appear more in $[\bar{1}12]$ Cu single crystals. However on the observation plane $(1\bar{1}1)$, $[459]$ Ag single crystals are filled with PSB walls, which is determined by the choice of the observed plane. Different observation planes reflect different profiles of the similar dislocation arrangements. The detailed discussion about dislocation profiles on different observation planes have been made elsewhere [25]. It should be pointed out that Jin et al. [9,10] observed two sets of two-phase structures composed of the primary and secondary slip systems in $[\bar{1}12]$ Cu single crystal. The primary $[\bar{1}01]$ ladders and conjugate $[011]$ ladders were found to be embedded in vein structures composed of dislocations with the appropriate Burgers vectors. Each independent set of PSB ladders is similar to those formed in single-slip oriented crystals. However, in this study, no conjugate $[011]$ ladders were found in both Cu and Ag single crystals. This is understandable because the operating of the secondary slip system is not an easy process, even for double-slip orientations. On the other hand, whether the secondary slip system has been activated does not affect the fact that two-phase structure is the classical dislocation structure in conjugate double-slip oriented fcc crystals. Combined with the CSS curves in Fig. 3(b), it can

be made sure that the formation of PSB ladders is directly related to the plateau region in fcc single crystals.

Critical double-slip oriented fcc crystals have different dislocation reaction models [9,10]. Fig. 7 shows the typical dislocation arrangements of these oriented Cu and Ag single crystals. Li et al. [43] found that at low strain amplitudes $[017]$ Cu single crystal is full of the vein structure. Different from single-slip oriented Cu single crystal these veins exhibit certain directivity, as shown in Fig. 7(a). When $\gamma_{pl} = 9.4 \times 10^{-4}$, it can be seen that the regular vein structure has formed. At the same time the traces of PSB ladders along the primary slip plane is still presented (see Fig. 7(b)). Jin et al. [9,10] had indicated that dislocation reactions between slip systems of $[\bar{1}01]$ (111) and $[101]$ $(\bar{1}\bar{1}\bar{1})$ led to the formation of sessile jogs. Because the intensity of dislocation reaction is not high, the majority of one type of dislocation in each zone constitutes a structure strongly affected by the dislocations of the other slip system. According to the degree of influence, structures in some zones may be PSB ladders similar to those in the single-slip oriented crystals, but in others they may be labyrinth-like. Fig. 7(c) and (d) gives the dislocation structure in $[\bar{1}414]$ Ag single crystals at different strain amplitudes. When $\gamma_{pl} = 1.0 \times 10^{-4}$, only primary slip system is running and the dislocation arrangements are composed of PSBs and veins. Likewise the vein structure shows some directivity. And when $\gamma_{pl} = 5.0 \times 10^{-4}$, an incomplete labyrinth-like structure can be formed by the interaction between the primary and critical slip systems. Compared with the conjugate double-slip orientations, the secondary slip system appears in the critical double-slip oriented single crystal much easily and even becomes dominant in some zones. By comparison of the experimental results, it can be proved that the dislocation configurations are slightly different between Cu and Ag single crystals because of the difference in orientations. PSB ladders can be seen in $[\bar{1}414]$ Ag single crystal, but only veins appear in $[017]$ Cu single crystal. Furthermore in their CSS curves, the plateau behavior appears in $[\bar{1}414]$ Ag single crystal; however no plateau can be seen in $[017]$ Cu single crystals. Finally at higher strain amplitudes, either for Cu or Ag, the observation plane of single crystals is covered by the labyrinth structure, which is much representative. In other words, when the orientation of Cu or Ag single crystals is closer to the criti-

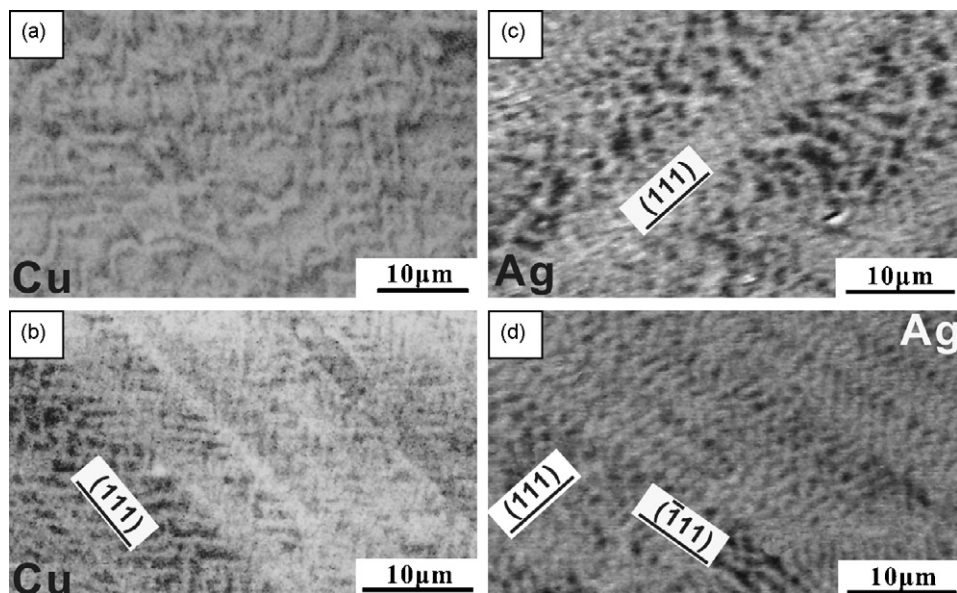


Fig. 7. Dislocation configurations of critical double-slip oriented Cu and Ag single crystals at different plastic strain amplitudes: (a) $[017]$ Cu single crystal cycled at $\gamma_{pl} = 1.2 \times 10^{-4}$, irregular labyrinth structure; (b) $[017]$ Cu single crystal cycled at $\gamma_{pl} = 9.4 \times 10^{-4}$, regular labyrinth and PSB-ladder structures; (c) $[\bar{1}414]$ Ag single crystal cycled at $\gamma_{pl} = 1.0 \times 10^{-4}$, irregular labyrinth and PSB-ladder structures; (d) $[\bar{1}414]$ Ag single crystal cycled at $\gamma_{pl} = 5.0 \times 10^{-4}$, regular labyrinth and PSB-ladder structures. (a) and (b) Viewed from $(\bar{2}7\bar{1})$ plane; (c) and (d) viewed from $(6\bar{2}\bar{1})$ plane. $[017]$ Cu single crystals are from Li et al. [43].

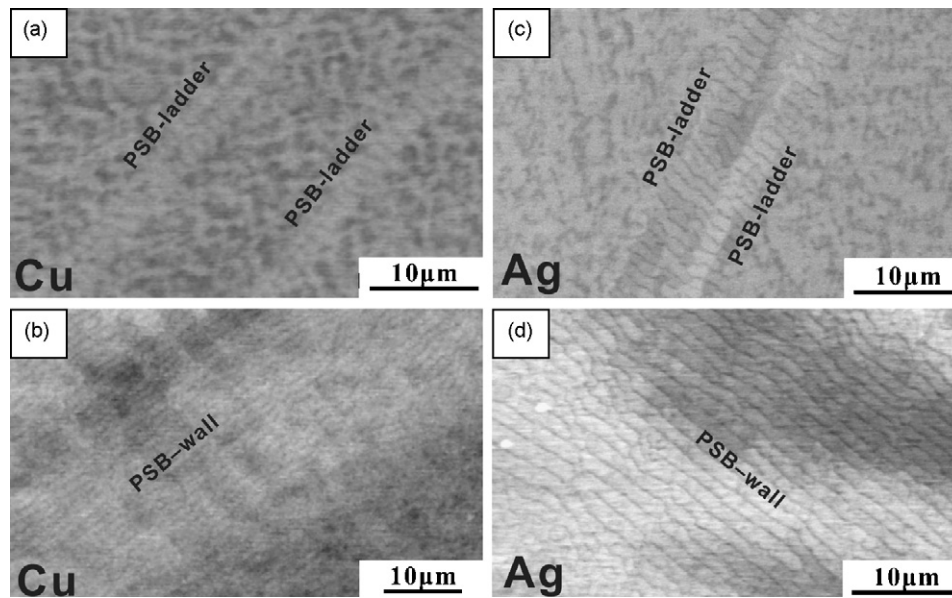


Fig. 8. Dislocation configurations of [0 1 1] multiple-slip oriented Cu and Ag single crystals at different plastic strain amplitudes: (a) $\gamma_{pl} = 6.1 \times 10^{-4}$; (b) $\gamma_{pl} = 1.22 \times 10^{-3}$; (c) $\gamma_{pl} = 6.1 \times 10^{-4}$; (d) $\gamma_{pl} = 3.7 \times 10^{-3}$. (a) and (b) Viewed from (1 2 2) and $(\bar{1} 2 \bar{2})$ planes, respectively; (c) and (d) viewed from (2 1 1) plane.

cal double-slip orientations, the labyrinth structure becomes much apparent.

[0 1 1] multiple-slip oriented Ag single crystal has four different slip systems. In this paper, we will try to summarize the features of their dislocation patterns by comparing the same [0 1 1] Cu and Ag single crystals. Fig. 8 provides the results of this comparison. It is clear that the appearance of PSB wall structure is the main feature. These walls are different from those walls observed on the (1 1 1) plane. It should be emphasized that the wall structure in Fig. 8(b) and (d) comes from the evolution of PSB ladders. Therefore, in [0 1 1] Cu and Ag single crystals, PSB bears most of the plastic deformation at low strain amplitude [18]. But with increasing the strain amplitude, the type II deformation band (DBII) that is composed of PSB wall structure will carry much plastic deformation. In this regard, Zhang et al. [44] had made sufficient discussion. They suggested that at high strain amplitude the original two-phase structure of PSBs and veins will be replaced by the new two-phase structure of DBII and PSBs in order to fulfill the redistribution of the plastic strain. So far, in [0 1 1] Cu and Ag single crystal PSB wall can be regarded as the most classical dislocation pattern in the cyclic saturation stage.

By comparing the CSS curves and dislocation arrangements of differently oriented Cu and Ag single crystals, the main features implied by the orientation effect can be summarized as below: (1) the obvious plateau behavior usually appears in single-slip, conjugate double-slip and [0 1 1] multiple-slip oriented Cu and Ag single crystals. The dislocation patterns of cyclic saturated Cu and Ag single crystals with these orientations are mostly composed of two-phase structure including PSBs and veins; (2) the coplanar double-slip oriented Cu and Ag single crystals do not show clear plateau region. Their saturation stresses gradually increase with increasing the strain amplitudes and are generally higher than those of single-slip oriented crystals. Meanwhile, the vein structure evolves into cell structure gradually, which is the prominent feature of such orientations; (3) the saturation stresses of critical double-slip oriented Cu and Ag single crystals are also higher than those of their respective single-slip oriented crystals. The labyrinth structure occurs eventually by the interaction between the primary and critical secondary slip systems. From the analysis above, a whole prospect about the orientation effect has been presented. The effect

of the orientation on the cyclic deformation behavior of Cu and Ag single crystals shows great similarities. These similarities are the key to answer the cyclic deformation behavior of fcc crystals, which needs further research and summarization.

4. Conclusions

- (1) Single-slip, conjugate double-slip and [0 1 1] multiple-slip oriented Cu and Ag single crystals show obvious plateau behavior in their CSS curves. The plateau stresses of Cu and Ag single crystals are 28 MPa and 20 MPa, respectively. Coplanar and critical double-slip oriented Cu and Ag single crystals do not exhibit clear plateau region. Their saturation stresses increase with increasing the strain amplitude.
- (2) In single-slip, conjugate double-slip and [0 1 1] multiple-slip oriented Cu and Ag single crystals, the dislocation patterns are mostly composed of two-phase structure including PSBs and veins. And only in [0 1 1] Cu and Ag single crystals, the PSB walls more than two-phase structure can be observed. These walls are different from the wall structure observed on the (1 1 1) plane and mainly located in the DBII of crystals. The dislocation patterns in critical double-slip oriented Cu and Ag single crystals are composed of the interaction between the primary and secondary slip systems. At higher strain amplitude, the above dislocation patterns will further evolve into the labyrinth structure. The cell structure usually appears in coplanar double-slip oriented Cu and Ag single crystals. Both labyrinth and cell structures are caused by the dislocation reaction, which is the basic reason why the plateau disappears.

Acknowledgements

The authors are grateful to Prof. H. Mughrabi and Prof. X.W. Li for sound suggestions and advices. Thanks are also due to H.H. Su, W. Gao, P. Zhang and H.F. Zou for their assistance in the fatigue experiments and dislocation observations. This work was financially supported by the "Hundred of Talents Project" of Chinese Academy of Sciences, the National Outstanding Young Scientist Foundation under Grant No. 50625103, and the National Basic Research Program of China under Grant No. 2010CB631006.

References

- [1] N. Thompson, N. Wadsworth, N. Louat, *Philos. Mag.* 1 (1956) 113.
[2] T. Broom, R.K. Ham, *Proc. R. Soc. Lond. A* 251 (1959) 186.
[3] O. Helgeland, *J. Inst. Metals* 93 (1965) 570.
[4] E.E. Laufer, W.N. Roberts, *Philos. Mag.* 14 (1966) 65.
[5] P.J. Woods, *Philos. Mag.* 28 (1973) 155.
[6] A.T. Winter, *Philos. Mag.* 30 (1974) 719.
[7] J.M. Finney, C. Laird, *Philos. Mag.* 31 (1975) 339.
[8] A.S. Cheng, C. Laird, *Mater. Sci. Eng.* 51 (1981) 111.
[9] N.Y. Jin, *Philos. Mag. A* 48 (1983) L33.
[10] N.Y. Jin, A.T. Winter, *Acta Metall.* 32 (1984) 989.
[11] N.Y. Jin, *Acta Metall. Sin.* 24 (1988) 299.
[12] N.Y. Jin, *Acta Metall. Sin.* 24 (1988) 311.
[13] B. Gong, Z.R. Wang, Z.G. Wang, *Acta Mater.* 45 (1997) 1365.
[14] B. Gong, Z.R. Wang, D.L. Chen, Z.G. Wang, *Scr. Mater.* 37 (1997) 1605.
[15] T.K. Lepisto, V.T. Kuokkala, P.O. Kettunen, *Scr. Metall.* 18 (1984) 245.
[16] T.K. Lepisto, P.O. Kettunen, *Mater. Sci. Eng.* 83 (1986) 1.
[17] T.K. Lepisto, V.T. Kuokkala, P.O. Kettunen, *Mater. Sci. Eng.* 81 (1986) 457.
[18] X.W. Li, Z.G. Wang, G.Y. Li, S.D. Wu, S.X. Li, *Acta Mater.* 46 (1998) 4497.
[19] X.W. Li, Z.G. Wang, S.X. Li, *Philos. Mag. Lett.* 79 (1999) 715.
[20] X.W. Li, Z.G. Wang, S.X. Li, *Philos. Mag. Lett.* 79 (1999) 869.
[21] X.W. Li, PhD Thesis, Institute of Metal Research, 1998.
[22] X.W. Li, Z.F. Zhang, Z.G. Wang, S.X. Li, Y. Umakoshi, *Defect Diffus. Forum* 188–190 (2001) 153.
[23] X.W. Li, Y. Umakoshi, S.X. Li, Z.G. Wang, *Z. Metallkd.* 92 (2001) 1222.
[24] X.W. Li, Y. Zhou, W.W. Guo, G.P. Zhang, *Cryst. Res. Technol.* 44 (2009) 315.
[25] P. Li, Z.F. Zhang, S.X. Li, Z.G. Wang, *Acta Mater.* 56 (2008) 2212.
[26] H. Mughrabi, *Mater. Sci. Eng.* 33 (1978) 207.
[27] X.W. Li, Z.G. Wang, S.X. Li, *Mater. Sci. Eng. A* 260 (1999) 132.
[28] X.W. Li, Z.G. Wang, S.X. Li, *Mater. Sci. Eng. A* 269 (1999) 166.
[29] X.W. Li, Z.G. Wang, S.X. Li, *Mater. Sci. Eng. A* 265 (1999) 18.
[30] P. Li, Z.F. Zhang, X.W. Li, S.X. Li, Z.G. Wang, *Acta Mater.* 57 (2009) 4845.
[31] R. Zauter, F. Petry, M. Bayerlein, C. Sommer, H.J. Christ, H. Mughrabi, *Philos. Mag. A* 66 (1992) 425.
[32] A. Schwab, J. Bretschneider, C. Buque, C. Blochwitz, C. Holste, *Philos. Mag. Lett.* 74 (1996) 449.
[33] D. Melisova, B. Weiss, R. Stickler, *Scr. Mater.* 36 (1997) 1061.
[34] J. Ahmed, A.J. Wilkison, S.G. Roberts, *Philos. Mag. A* 81 (2001) 1473.
[35] Z.F. Zhang, Z.G. Wang, *Philos. Mag. Lett.* 78 (1998) 105.
[36] Z.F. Zhang, Z.G. Wang, *Philos. Mag. A* 79 (1999) 741.
[37] Z.F. Zhang, Z.G. Wang, *Philos. Mag. A* 81 (2001) 399.
[38] D.L. Chen, D. Melisova, B. Weiss, R. Stickler, *Fatigue Fract. Eng. M* 20 (1997) 1551.
[39] Z.X. Tong, J.P. Baiulon, *Fatigue Fract. Eng. M* 18 (1995) 847.
[40] H. Mughrabi, Unpublished data of 1979, Private Communication, 2008.
[41] P. Li, Z.F. Zhang, S.X. Li, Z.G. Wang, *Philos. Mag.* 89 (2009) 2903.
[42] Y. Zhou, MS Thesis, Northeastern University, 2008.
[43] X.W. Li, Y. Umakoshi, B. Gong, S.X. Li, Z.G. Wang, *Mater. Sci. Eng. A* 333 (2002) 51.
[44] Z.F. Zhang, Z.G. Wang, Z.M. Sun, *Acta Mater.* 49 (2001) 2875.